

Midinfrared intersubband absorption in $\text{Zn}_x\text{Cd}_{1-x}\text{Se}/\text{Zn}_{x'}\text{Cd}_{y'}\text{Mg}_{1-x'-y'}\text{Se}$ multiple quantum well structures

H. Lu, A. Shen, and M. C. Tamargo^{a)}

Department of Chemistry, The City College of the City University of New York, New York, New York 10031

C. Y. Song and H. C. Liu

Institute for Microstructural Sciences, National Research Council, Ottawa K1A 0R6, Canada

S. K. Zhang and R. R. Alfano

Institute for Ultrafast Spectroscopy and Lasers, Department of Physics, The City College of The City University of New York, New York, New York 10031

M. Muñoz

Department of Physics, Virginia Commonwealth University, Richmond, Virginia 23284

(Received 16 May 2006; accepted 23 August 2006; published online 25 September 2006)

The authors report the observation of intersubband absorption in $\text{Zn}_x\text{Cd}_{(1-x)}\text{Se}/\text{Zn}_{x'}\text{Cd}_{y'}\text{Mg}_{(1-x'-y')}\text{Se}$ multiple quantum wells. Lattice-matched samples were grown by molecular beam epitaxy on InP (001) substrates. Photoluminescence measurements indicate that the samples have excellent material quality. The peak absorption wavelengths measured by Fourier transform infrared spectroscopy are 3.99 and 5.35 μm for two samples with $\text{Zn}_x\text{Cd}_{(1-x)}\text{Se}$ well widths of 28 and 42 \AA , respectively. These values fall within the 3–5 μm wavelength range, which is of interest for midinfrared intersubband devices, such as quantum cascade lasers and quantum well infrared photodetectors. Their experimental results fit well with theoretical predictions based on the envelope function approximation. The results indicate that these wide band gap II-VI materials are very promising for midinfrared intersubband device applications. © 2006 American Institute of Physics. [DOI: 10.1063/1.2354578]

Devices based on intersubband (ISB) transitions, such as quantum cascade lasers (QCLs) and quantum well (QW) infrared photodetectors, are being extensively studied due largely to their potential applications.¹ Most of the ISB devices demonstrated so far have been fabricated with III-V compound semiconductors.^{2,3} Band structure engineering has made it possible to achieve ISB devices operating over a wide spectrum range without the need to change the material system. For example, QCLs that emit in a very wide wavelength range ($\sim 3.4\text{--}24\ \mu\text{m}$) have been realized with InP-based InGaAs/InAlAs material system^{4,5} after the first demonstration by Faist *et al.* in 1994.⁶ However, most of these demonstrated devices can only be performed at cryogenic temperature with pulsed operation mode and relatively low power outputs. So far, the shortest wavelength that has been achieved for a QCL operating at room temperature (RT) is $\sim 4\ \mu\text{m}$ with a strain compensated InGaAs/InAlAs heterostructure.⁷ One of the reasons why it is difficult to achieve RT short wavelength operation is the limited conduction band offset (CBO) of the heterostructures used. For some applications such as trace gas sensing, infrared lasers with wavelength shorter than 4 μm operating at RT are required.^{2,8} To achieve QCLs operating at high temperature with a shorter emission wavelength, materials with larger CBO must be used. One approach to achieve the larger CBO is to use the type-II band alignment in InAs/AlSb, InGaAs/AlAsSb,^{9–11} and (CdS/ZnSe)/BeTe.^{12,13} However, the growth of these materials is more difficult, due to the

lack of common ions, and the type-II structure may introduce additional complications in the operation of the device. The only effort on achieving shorter wavelength devices with a material having a type-I band alignment has been with the wide band gap GaN/AlGaIn system.^{14–17} Although ISB absorption in QWs at wavelength as short as 1.08 μm has been observed,¹⁸ the poor material quality (high defect density and poor interfacial quality due to the lack of lattice-matched substrate) makes it very difficult to realize a practical working device.

We propose that a wide band gap II–VI material system, $\text{Zn}_x\text{Cd}_{(1-x)}\text{Se}/\text{Zn}_{x'}\text{Cd}_{y'}\text{Mg}_{(1-x'-y')}\text{Se}$, which has a large CBO with a type-I band alignment and can be grown lattice matched on InP substrates, is a very promising candidate for realizing shorter wavelength ISB devices operating at RT. By simply changing the composition, the band gap of the barrier layer, $\text{Zn}_{x'}\text{Cd}_{y'}\text{Mg}_{(1-x'-y')}\text{Se}$, can be tuned continuously from 2.1 to 3.6 eV.¹⁹ Red-green-blue full color light emitting diodes and photopumped lasers have been demonstrated by using this material system.^{20–22} Contactless electroreflectance measurements reveal that a CBO as large as 1.12 eV can be achieved in the material system.²³

In this letter, we report the observation of ISB absorption in $\text{Zn}_x\text{Cd}_{(1-x)}\text{Se}/\text{Zn}_{x'}\text{Cd}_{y'}\text{Mg}_{(1-x'-y')}\text{Se}$ multiple quantum wells (MQWs) lattice matched to InP substrates. For two samples with $\text{Zn}_x\text{Cd}_{(1-x)}\text{Se}$ well widths of 28 and 42 \AA and a $\text{Zn}_{x'}\text{Cd}_{y'}\text{Mg}_{(1-x'-y')}\text{Se}$ barrier band gap of 2.9 eV, peak absorption wavelengths at 3.99 and 5.35 μm , respectively, were observed.

^{a)} Author to whom correspondence should be addressed; electronic mail: tamar@sci.cuny.cuny.edu

The samples were grown by molecular beam epitaxy (MBE) on (001) semi-insulating InP in a dual-chamber Riber 2300P MBE system. After the removal of oxide layer and the growth of a 0.15 μm InGaAs buffer layer in the III-V growth chamber, the samples were transferred through vacuum modules to the II-VI growth chamber. The InGaAs surface was exposed to a Zn flux for 10 s followed by the growth of a 10 nm ZnCdSe buffer layer at 200 $^{\circ}\text{C}$. The substrate temperature was then raised to 300 $^{\circ}\text{C}$ to grow the subsequent layers. To ensure the lattice matching of both the $\text{Zn}_x\text{Cd}_{(1-x)}\text{Se}$ wells and the $\text{Zn}_{x'}\text{Cd}_{y'}\text{Mg}_{(1-x'-y')}\text{Se}$ barriers to the InP substrate, two Zn cells were employed. The two samples reported here consist of 80 periods (sample A) and 60 periods (sample B) of $\text{Zn}_x\text{Cd}_{(1-x)}\text{Se}/\text{Zn}_{x'}\text{Cd}_{y'}\text{Mg}_{(1-x'-y')}\text{Se}$ multiple quantum wells. The $\text{Zn}_x\text{Cd}_{(1-x)}\text{Se}$ well thickness was 28 \AA for sample A and 42 \AA for sample B. The well had the lattice-matched composition, $x=0.46$, and was doped with Cl (using ZnCl_2 as dopant source) to $2 \times 10^{18} \text{ cm}^{-3}$. The $\text{Zn}_{x'}\text{Cd}_{y'}\text{Mg}_{(1-x'-y')}\text{Se}$ barrier thickness was about 100 \AA in both samples. The Zn and Cd contents in the $\text{Zn}_{x'}\text{Cd}_{y'}\text{Mg}_{(1-x'-y')}\text{Se}$ were $x'=0.24$ and $y'=0.25$, respectively, corresponding to a band gap of 2.9 eV at RT. The MQWs were sandwiched between a 0.3 μm bottom and a 0.1 μm cap $\text{Zn}_x\text{Cd}_{(1-x)}\text{Se}$ layers. The growth rate and doping concentration were determined from separate calibration layers. These layers were also grown to optimize the growth conditions. The results obtained from double-crystal x-ray diffraction rocking curve measurements indicate the excellent structural quality of the samples.²⁴

Photoluminescence (PL) measurements were carried out at 77 K and room temperature with the UV line (325 nm) of a He-Cd laser as the excitation source. For ISB absorption measurements, the samples were polished to a multiple-pass waveguide geometry with parallel 45 $^{\circ}$ facets [see the inset of Fig. 2(a)]. The absorption measurements were performed at RT using a Bomem MB-100 Fourier transform infrared (FTIR) spectrometer. A cooled HgCdTe detector was used.

Figure 1(a) shows the PL spectra of the two samples at 77 K. Sharp peaks from the MQWs can be seen from both samples with no traces of any deep level emissions. The peak at ~ 568 nm is the emission from the $\text{Zn}_x\text{Cd}_{(1-x)}\text{Se}$ cap layer. The full widths at half maximum (FWHMs) of the PL emission peaks of the two samples are 40 and 42 meV, an evidence of good material quality. As shown in Fig. 1(b), a well-behaved quantum shift is observed, as the PL emission moves to higher energy with the decrease of well width. In Fig. 1(b), the solid line is the calculated transition energy as a function of well width, based on the envelope function approximation. Excellent agreement between the calculated transition energies and the experimental results is observed. In the calculations we assumed that $Q_c=0.80$ determined in our previous study,²⁵ where $Q_c=\Delta E_c/\Delta E_g$ is the fraction of the band gap difference ΔE_g that is in the conduction band. The band gaps of the $\text{Zn}_{x'}\text{Cd}_{y'}\text{Mg}_{(1-x'-y')}\text{Se}$ barrier and $\text{Zn}_x\text{Cd}_{(1-x)}\text{Se}$ well were determined from calibration layers. The calculation of the effective masses was carried out in the same way that was described in Ref. 25.

Figure 2(a) shows the normalized absorbance of the samples at room temperature. The spectra were obtained by taking the ratio of *P*-polarized spectra over *S*-polarized spectra. For samples A and B with well widths of 28 and 42 \AA , peak absorptions λ_p at 3.99 μm (0.31 eV) and 5.35 μm

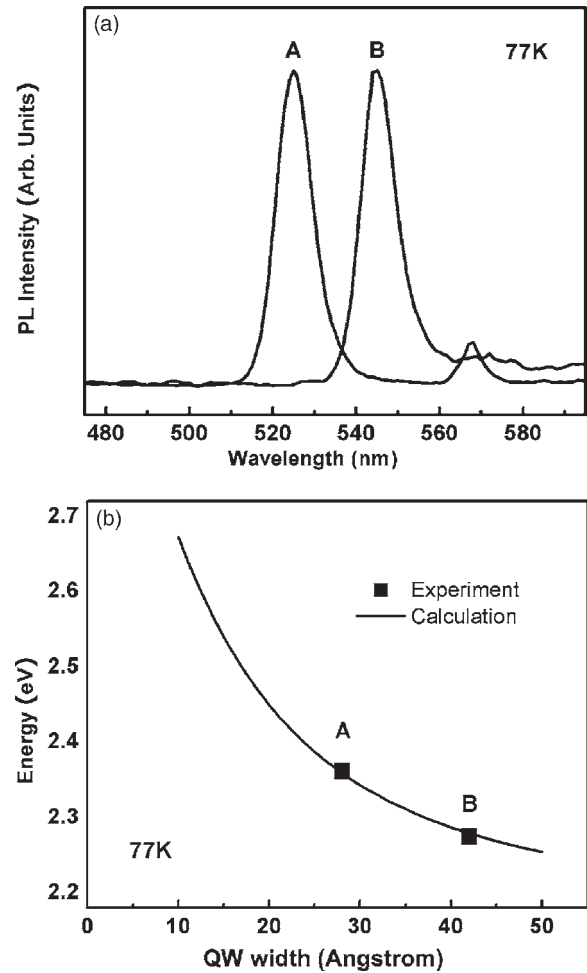


FIG. 1. (a) 77 K PL spectra of two MQW samples with different QW widths: 28 \AA for sample A and 42 \AA for sample B. (b) The E1-H1 interband transitions as a function of QW width calculated using envelope function approximation. A contribution of 80% of the band gap difference to the conduction band is assumed. The experimental data are indicated by the square dots, which fit well with the theoretical calculation.

(0.23 eV), respectively, were obtained. The absolute absorption for sample A is about 75%. Taking into account the dimension of the waveguide sample, a single pass absorption of 4.6% is obtained. Fitting by a Gaussian line shape gives the FWHM (ΔE) values of 55 and 28 meV for the two samples. For both samples, $\Delta E/E_{\text{peak}}$ is of the order of 10%, which is typical for a bound-to-bound transition and comparable to the values obtained for the well-studied III-V semiconductors.¹ For sample B, a second, weaker absorption peak is seen at ~ 0.5 eV. We tentatively attribute this peak to the bound-to-continuum absorption in the well, but additional work is needed to confirm this assignment.

The peak absorption wavelength as a function of QW width was plotted in Fig. 2(b). The lines are the theoretical curves obtained from the envelope function approximation calculation for slightly different values of Q_c . The values of the band gaps of the barrier and the well used in the calculation were obtained from the 77 K PL emission of the calibration layers. A 70 meV correction is made to obtain the room-temperature values. The experimental data are in good agreement with the predicted values within the range of Q_c . It suggests that for the barrier composition used in this study it would be difficult to achieve shorter wavelength by simply reducing the QW width. Further reduction of the absorption

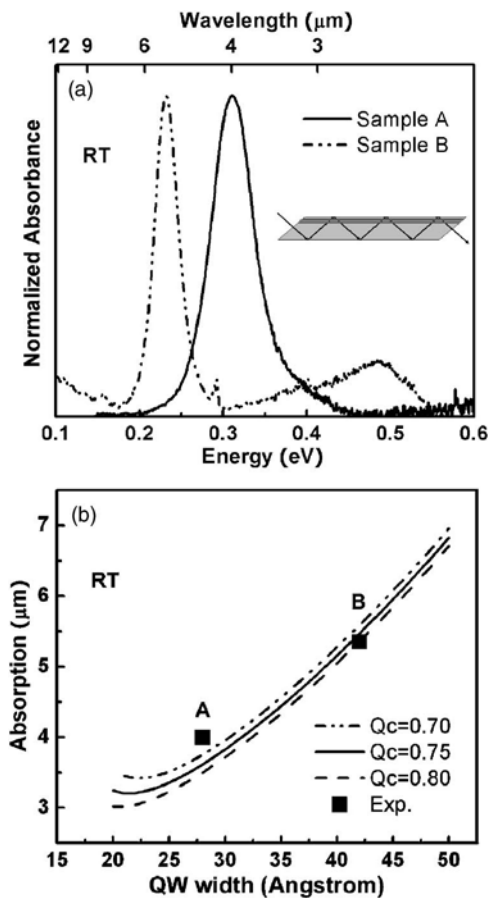


FIG. 2. (a) Normalized absorbance from the MQW samples A and B measured by FTIR at RT. The spectrum is the ratio of *P*-polarized light over *S*-polarized light through a multipass waveguide geometry of the sample [inset of (a)]. (b) The theoretical calculations of the ISB absorption wavelength as a function of QW width with different Q_c values. The square dots represent the experimental data from the FTIR measurement on samples A and B.

wavelength might be possible if a wider band gap barrier layer is used. A maximum band gap of 3.6 eV can be obtained with this material system. Also, the use of strain compensated structures may result in shorter wavelength devices.

In conclusion, we report the observation of ISB transitions in wide band gap $\text{Zn}_{0.46}\text{Cd}_{0.54}\text{Se}/\text{Zn}_{0.24}\text{Cd}_{0.25}\text{Mg}_{0.51}\text{Se}$ MQWs. The lattice-matched samples were grown on InP substrates by MBE. PL measurements demonstrate that the samples have excellent material quality. For two samples with well widths of 28 and 42 Å, peak absorptions at 3.99 μm (0.31 eV) and 5.35 μm (0.23 eV) and FWHMs of 55 and 28 meV were obtained. The experimental data are in good agreement with theoretical predictions. By further decreasing the well width and increasing the band gap of the $\text{Zn}_x\text{Cd}_y\text{Mg}_{(1-x-y)}\text{Se}$ barrier layer, ISB transitions at even shorter wavelength are expected. These results indicate that

$\text{Zn}_x\text{Cd}_{(1-x)}\text{Se}/\text{Zn}_x\text{Cd}_y\text{Mg}_{(1-x-y)}\text{Se}$ is a very promising material system for ISB devices operating in the midinfrared spectral range between 3 and 5 μm .

This work was supported by NSF Grant No. ECS0217646 and NASA Grant No. NCC-1-03009.

¹Intersubband Transitions in Quantum Wells: Physics and Device Applications I & II, Semiconductors and Semimetals Vols. 62 and 66, edited by H. C. Liu and F. Capasso (Academic, San Diego, 2000).

²Claire Gmachl, Federico Capasso, Deborah L. Sivco, and Alfred Y. Cho, Rep. Prog. Phys. **64**, 1533 (2001).

³B. F. Levine, J. Appl. Phys. **74**, R1 (1993).

⁴Jerome Faist, Federico Capasso, Deborah L. Sivco, Albert L. Hutchinson, Sung-Nee G. Chu, and Alfred Y. Cho, Appl. Phys. Lett. **72**, 638 (1998).

⁵Raffaële Colombelli, Federico Capasso, Claire Gmachl, Albert L. Hutchinson, Deborah L. Sivco, Alessandro Tredicucci, Michael C. Wanke, A. Michael Sergent, and Alfred Y. Cho, Appl. Phys. Lett. **78**, 2620 (2001).

⁶Jerome Faist, Federico Capasso, Deborah L. Sivco, Carlo Sirtori, Albert L. Hutchinson, and Alfred Y. Cho, Science **264**, 553 (1994).

⁷J. S. Yu, S. R. Darvish, A. Evans, J. Nguyen, S. Slivken, and M. Razeghi, Appl. Phys. Lett. **88**, 041111 (2006).

⁸A. Evans, J. S. Yu, J. David, L. Doris, K. Mi, S. Slivken, and M. Razeghi, Appl. Phys. Lett. **84**, 314 (2004).

⁹R. Teissier, D. Barate, A. Vicet, C. Alibert, A. N. Baranov, X. Marcadet, C. Renard, M. Garcia, C. Sirtori, D. Revin, and J. Cockburn, Appl. Phys. Lett. **85**, 167 (2004).

¹⁰D. G. Revin, L. R. Wilson, E. A. Zibik, R. P. Green, J. W. Cockburn, M. J. Steer, R. J. Airey, and M. Hopkinson, Appl. Phys. Lett. **85**, 3992 (2004).

¹¹Q. Yang, C. Manz, W. Bronner, Ch. Mann, L. Kirste, K. Koehler, and J. Wagner, Appl. Phys. Lett. **86**, 131107 (2005).

¹²R. Akimoto, B. S. Li, K. Akita, and T. Hasama, Appl. Phys. Lett. **87**, 181104 (2005).

¹³Ryoichi Akimoto, Bing Sheng Li, Fumio Sasaki, and Toshifumi Hasama, Jpn. J. Appl. Phys., Part 1 **43**, 1973 (2004).

¹⁴Claire Gmachl, Hock M. Ng, and Alfred Y. Cho, Appl. Phys. Lett. **77**, 334 (2000).

¹⁵Norio Lizuka, Kei Kaneko, and Nobuo Suzuki, Appl. Phys. Lett. **81**, 1803 (2002).

¹⁶C. Gmachl, H. M. Ng, S.-N. George Chu, and Alfred Y. Cho, Appl. Phys. Lett. **77**, 3722 (2000).

¹⁷A. Vardi, N. Akopian, G. Bahir, L. Doyennette, M. Tchernycheva, L. Nevou, F. H. Julien, F. Guillot, and E. Monroy, Appl. Phys. Lett. **88**, 143101 (2006).

¹⁸Katsumi Kishino, Akihiko Kikuchi, Hidekazu Kanazawa, and Tetsuo Tachibana, Appl. Phys. Lett. **81**, 1234 (2002).

¹⁹S. P. Guo and M. C. Tamargo, in *II-VI Semiconductor Materials and their Applications*, edited by M. C. Tamargo (Taylor & Francis, New York, 2002), Vol. 12, pp. 261–286.

²⁰Y. Guo, G. Aizin, Y. C. Chen, L. Zeng, A. Cavus, and M. C. Tamargo, Appl. Phys. Lett. **70**, 1351 (1997).

²¹L. Zeng, Y. Guo, B. X. Yang, A. Cavus, W. Lin, Y. Y. Luo, Y. C. Chen, and M. C. Tamargo, Appl. Phys. Lett. **72**, 3136 (1998).

²²M. C. Tamargo, W. Lin, S. P. Guo, Y. Luo, Y. Guo, and Y. C. Chen, J. Cryst. Growth **214/215**, 1058 (2000).

²³Mohammad Sohel, Xuecong Zhou, Hong Lu, M. Noemi Perez-Paz, Maria Tamargo, and Martin Muñoz, J. Vac. Sci. Technol. B **23**, 1209 (2005).

²⁴H. Lu, A. Shen, M. Muñoz, M. N. Perez-Paz, M. Sohel, S. K. Zhang, R. R. Alfano, and M. C. Tamargo, Phys. Status Solidi B **243**, 868 (2006).

²⁵Martin Muñoz, Hong Lu, Xuecong Zhou, Maria C. Tamargo, and Fred H. Pollak, Appl. Phys. Lett. **83**, 1995 (2003).